3D Face recognition Robust to Expression Occlusion and Poses

Miss Ashwini S Gavali
Dept. Comp.science and IT
Dr.B.A.M.U,Aurangabad

Prof. Ratnadeep.R.Deshmukh
Dept. Comp.science and IT,
Dr.B.A.M.U,Aurangabad

***Abstract**:* Face recognition has numerous applications in various identification and authentication system, but the accuracy of face recognition decreases in presence of large facial expression, occlusion and pose variations. This paper illustrates the use of scale invariant feature transform (SIFT) on 3D meshes to mode facial deformation caused by expression, occlusion and variation in poses. Here we used meshSIFT algorithm for feature extraction and sparse representation classifier for feature matching. Given a 3D face scan, its descriptors are extracted at first and then its identity can be determined by using sparse representation classifier. The proposed 3D face recognition system is robust to challenges such as large facial expressions (especially those with open mouths), large pose variations, missing parts, and partial occlusions due to glasses, hair, and so on. Our results is verified on Bosphorus Database, and I got approximate 92.46%accuracy on Bosphorus dataset.

***Keywords**: feature extraction; feature matching; scale invariant feature transform; sparse representation classifier;*

I INTRODUCTION

Face is one of the popular biometric identities of person. Each person in the world has different appearance. Due to these variations in face, face is the most widely accepted biometric modality. Our face is used in identity proof like passport, visa, license, voting card, ID, PAN card, Aadhar card etc. Along with that automated human face recognition has number of applications in variety of fields including automated secured access to ATM machines and buildings, automatic surveillance, forensic analysis, fast retrieval of records from databases in police departments, automatic identification of patients in hospitals, checking for fraud or identity theft, and human-computer interaction.

Due to this fact from last few decades a face recognition system becoming very useful in a variety of applications. There are number of biometric systems exists, such as fingerprints, gait, DNA, hand geometry, retina scan, ear, teeth etc. While some of these biometric recognition systems, such as fingerprints and iris, have already reached very high level of accuracy, but they have a limited use in non-cooperative scenarios. On the other hand, as face recognition is convenient but has not reached the desired levels of accuracy. Over the past three decades, the techniques for face recognition have received a growing attention within the computer vision community.

- *Ashwini S Gavali is currently pursuing masters degree program in Computer Science and engineering in Dr. B.AM.U .University, Aurangabad, Maharashtra, India, E-mail: ashugavli22@gmail.com.*
- *Ratnadeep R Deshmukh is currently working as Professor and Head in Department of Computer Science and Engineering, Dr. B.AM.U .University, Aurangabad, Maharashtra, India*

From last two decade most of the research has directed their attention towards developing reliable automatic face recognition systems that use two dimensional (2D) facial images. Commercial systems are also now available for 2D face recognition. But, two dimensional face recognition systems are inadequate for robust face recognition as 2D color imaging has some disadvantages like nuisance variables, such as illumination and small pose changes, have a relatively greater influence on the observations. Three dimensional facial images have some advantages over 2D facial images. As 3D image can be rotated so it is possible easily correct pose by rigid rotations in 3D space. Also images acquired using 3D laser range finders are invariant to illumination conditions during image acquisition. 3 dimensional facial images can also provide structural information about the face (e.g., surface curvature and geodesic distances), which cannot be obtained from a single 2D image. As more features can be made available by using 3D scan, it is possible to develop robust 3D face recognition system.

However, 3D scans often suffer from the problem of missing parts due to self-occlusions or external occlusions or some imperfections in the scanning technology. Additionally, variations in face scans due to changes in facial expressions can also degrade face recognition performance. To be useful in real-world applications, a 3D face recognition approach should be able to handle these challenges, i.e., it should recognize people despite large facial expression, occlusion and pose variations [1].

II. LITERATURE SURVEY

In this section we have listed various existing approaches for 3D face recognition that I studied to carry out this research.

Bronstein [2] use changes in surface distances with the Euclidean distances between corresponding points on a canonical face surface as a features.. To handle the open mouth problem, they first detect and remove the lip region, and then compute the surface distance in the presence of a hole corresponding to the removed part. The assumption of preservation of surface distances under facial expressions motivates several authors to define distance-based features for facial recognition.

Samir [2] use the level curves of the surface distance function (from the tip of the nose) as features for face recognition. Since an open mouth affects the shape of some level curves, this method is not able to handle the problem of missing data due to occlusion or pose variations.

Bronstein AM [4] where the study local geometric attributes under this parameterization. To deal with the open mouth problem, they modify the parameterization by disconnecting the top and bottom lips. The main limitation of this approach is the need for detecting the lips.

Lee [5] use ratios of distances and angles between eight fiducial points, followed by an SVM classifier.

Gupta [6] use Euclidean/geodesic distances between anthropometric fiducial points in conjunction with linear classifiers. As stated earlier, the problem of automated detection of fiducial points is nontrivial and hinders automation of these methods. This paper presented a systematic procedure for selecting facial fiducial points associated with diverse structural characteristics of a human face.

Faltemier et al. [7] use 38 face regions that densely cover the face, and fuse scores and decisions after performing ICP on each region.

Gordon [8] argues that curvature descriptors have the potential for higher accuracy in describing surface features and are better suited to describing the properties of faces in areas such as the cheeks, forehead, and chin. These descriptors are also invariant to viewing angles.

McKeon and Russ et al. [9] use a region ensemble approach that is based on Fisherfaces, i.e., face representations are learned using Fisher's discriminate analysis. This investigation is conducted using 3D Fisherfaces and demonstrates that region ensembles improve the ability of the Fisherface approach to create discriminating features, even for untrained subject samples. In fact, comparable performance can be achieved using significantly fewer training subjects.

Kakadiaris [10] utilize an annotated face model to study geometrical variability across faces. The annotated face model is deformed elastically to fit each face, thus matching different anatomical areas such as the nose, eyes, and mouth.

Queirolo [11] use surface interpenetration measure as a similarity measure to match two face images. The authentication score is obtained by combining the SIM values corresponding to the matching of four different face regions: circular and elliptical areas around the nose, forehead, and the entire face region.

Alyuz [12] proposed a new 3D face registration and recognition method based on local facial regions that is able to provide better accuracy in the presence of expression variations and facial occlusions. Proposed fast and flexible alignment method uses average regional models (ARMs), where local correspondences are inferred by the iterative closest point (ICP) algorithm. Dissimilarity scores obtained from local regional matchers are fused to robustly identify probe subjects.

Berretti [13] used surface distances to extract equal-width iso-geodesic facial stripes, which in turn, were used as nodes in a graph-based recognition algorithm. However, this approach are not able to deal with the problems caused by missing data or occlusions, since under these cases the shape of the level curves will definitely be affected. The approach takes into account geometrical information of the 3D face and encodes the relevant information into a compact representation in the form of a graph. Nodes of the graph represent equal width isogeodesic facial stripes.

Mahoor and Abdel-Mottaleb [14], represent each range image by ridge lines on the 3D surface of the face using a 3D binary image, namely ridge image, which is the locus of the points which have principal curvatures grater than a threshold. With respect to the matching strategy, they also resorted to ICP. The limitation of [40] lies in that it can only deal With frontal or near-frontal range scans.

Drira [15], represent facial surfaces by radial curves emanating from the nose tips and use elastic shape analysis of those curves to develop a Riemannian framework for analyzing shapes of full facial surfaces.

Jain [16] used the ICP algorithm to align 3D meshes containing face geometry. Their algorithm is based on four main steps: feature point detection in the probe images, rough alignment of probe to gallery by moving the probe centroid to match, iterative adjustment based on the closest point matching (ICP), and using known points (i.e. the eyes, tip of the nose and the mouth) to verify the match.

Chang [17] use multiple overlapping nose regions and obtain increased performance relative to using one whole-frontal-face region. These regions include a nose circle, nose ellipse, and a region composed of just the nose itself. This method uses the ICP algorithm to perform image matching.

Passalis [18] use automatic landmarking to estimate the pose and to detect occluded areas. The facial symmetry is used to overcome the challenges of missing data here.

Lu and Jain. [19] use manual landmarks to develop a thin-plate-spline-based matching of facial surfaces. A strong limitation of this approach is that the extraction of fiducial landmarks needed during learning is either manual or semi-automated

ISSN 2229-5518

IV. PROPOSED SYSTEM

Our approach is based on the meshSIFT algorithm [21] which is an extension of Scale Invariant Feature Transform (SIFT) proposed by David Lowe [20]. and is able to perform robust 3D face recognition in presence of large facial expression, occlusion and pose variations. The mesh-SIFT is an alignment free approach means it does not require pre alignment between two face scan as in approaches presented in literature. It can extracts features, ranging from fine details to coarse characteristic structures, in a shape-based scale space representation of the surface. The idea behind a scale space representation is to separate the structures in the surface according to the scale of the structure. This assumes that new structures must not be created from a fine to any coarser scale.

The overall pipeline of proposed system is depicted in fig 1.

In our approach, firstly for each 3D face scan n multiple keypoints are detected by using scale space extrema and then for each keypoint its local descriptor is extracted from histogram of its canonical orientation. The set of local descriptors of all keypoints of each scan is used as a representation of f. The gallery dictionary is created by concatenating all the local descriptors extracted from gallery samples. Given a probe face scan, its features are extracted first and then these features are matched with gallery scan using multi-task sparse classifier.

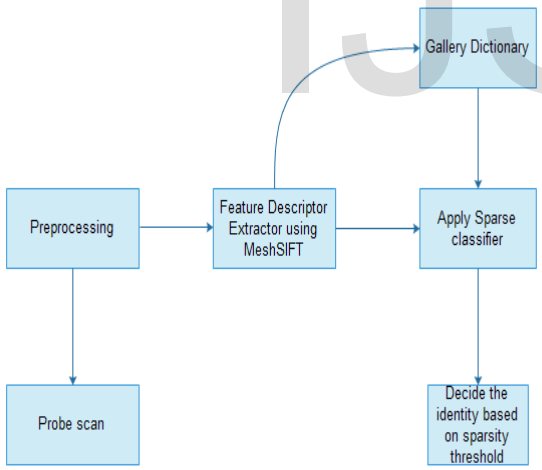

Fig 1: Overall pipeline of proposed system

V. FEATURE EXTRACTION USING meshSIFT

meshSIFT is efficient Method to extract and describe distinctive image features that are invariant to image scale and rotation. It is robust against change of viewpoint, noise and illumination change.

The basic steps of scale invariant feature transforms for 3D meshes (meshSIFT) are:

1. Keypoint localization
2. Orientation assignment
3. Keypoint descriptor

A. Keypoint localization

This is the stage where the interest points, which are called keypoints in the SIFT framework, are detected. For this, the image is convolved with Gaussian filters at different scales, and then the difference of successive Gaussian-blurred images is taken. Keypoints are then taken as maxima/minima of the Difference of Gaussians (DoG) that occur at multiple scales.

The mesh-SIFT algorithm starts from a surface mesh M= (V, E, T), consisting of a collection of vertices V = {v1 . . . v|V|} connected by edges E and a set of simplices T = {t1, . . . , t|T |} covering the surface such that T = ∪ti, ti∩tj = ∅ for i = j. Let N be a neighbourhood system defined on V, where Ni = {vj ∈ V| (vi, vj) ∈E} denotes the set of neighbourhood.

To detect The keypoint, a scale space is constructed containing smoothed versions of the input mesh Ms, expressed as

$$\begin{cases} Ms = 0 \\ \hat{G}_{\sigma_s} \otimes \text{Melse} \end{cases} \quad (1)$$

Where M_s is the original mesh and $\hat{G}_{\sigma_s}$ the approximated Gaussian filter with scale σ_s (standard deviation). These scales σ_s vary exponentially as $\sigma_s = 2^{\frac{s}{k}}.\sigma_0$ with k and σ_s parameters of the meshSIFT algorithm.

The Gaussian filter for meshes is approximated as sub-sequent convolutions of the mesh with a binomial filter. This binomial filter moves each vertex The Gaussian filter for meshes is approximated as sub- sequent convolutions of the mesh with a binomial filter. This binomial filter moves each vertex vi towards Vi towards

$$V_i^s = \frac{1}{|N_i|}(V_i + \sum_{j \in N_i} V_j) \quad (2)$$

Since the number of convolutions is discrete, σ_s is approximated as

$$\hat{\sigma}_s = \bar{e}.\sqrt{\frac{2.\sigma_0}{3}}.2^{\frac{s}{k}} \quad (3)$$

to approximate as close as possible the desired exponential behavior, with $\bar{e}$ the average edge length and s = 0 . . . n scales + 2.

Next, for the detection of salient points in the scale space, the mean curvature H is computed (using [20]) for each vertex i and at each scale s in the scale space,

$$H_i^s = \frac{K_{i,1}^s + K_{i,2}^s}{2} \quad (4)$$

(with $K_{i,1}^s$ and $K_{i,2}^s$ the maximal and minimal curvature in vertex i at scale s). Note that also other functions can be

defined on the mesh, such as the Gaussian curvature K, the shape index S (5) or the curvedness $C = \sqrt{2H^2 - k}$ The mean curvature, however, appeared to provide the most stable keypoints for 3D face data. Note also that the mesh itself is smoothed and not the function on the mesh. As such, meshSIFT better describes the shape's geometry. It is, however, not completely intrinsic anymore (and therefore, not completely invariant for local isometric deformations). Differences between subsequent scales are computed,

$$dH_i^s = H_i^{s+1} - H_i^s$$

and extrema (minima and maxima) in this scale space are selected as local feature locations. This means that each vertex with a higher (or lower) value of dH_i^s than all of its neighbours on the same scale as well as on the upper and lower scale is selected as keypoint. Finally, the scale σ_s at which this extremum is obtained is assigned to each key point.

B. Orientation Assignment

In order to obtain an orientation-invariant descriptor, each keypoint is assigned a canonical orientation. It allows, together with the normal to the surface at the keypoint, to construct a local reference frame in which the vertices of the neighbourhood can be expressed independent of the (facial) pose. By expressing the neighbourhood size as a $9\sigma_s$ function of the scale σ_s, we ensure a scale invariant descriptor as well. Only vertices within a spherical region with radius $9\sigma_s$ around each keypoint are considered. First, for each vertex within this (neighbourhood) region, the normal vector is computed and the geodesic distance to the respective keypoint is determined based on the fast marching algorithm for triangulated domains. Next, all calculated normal vectors in the neighbourhood are projected onto the tangent plane to the mesh containing the keypoint. These projected normal vectors are gathered in a weighted histogram comprising 360 bins (thus covering 360 degrees with a bin width of 1 degree). Each histogram entry is Gaussian weighted with its geodesic distance to the key- point, with a bandwidth proportional to the assigned scale(σ =4.5σ_s)The resulting histogram is smoothed by convolving it three times with a Gaussian filter (17 bins,σ = 17) for a more robust localization of the canonical orientation. Finally, the highest peak in the histogram and every peak above 80% of this highest peak value are selected as canonical orientations. By fitting a quadratic function to the histogram using the neighbouring bins of a peak, the canonical orientation is calculated to sub-bin precision. If more than one canonical orientation exists for a keypoint, this result in multiple keypoints, each as- signed one of the canonical orientations. Intuitively, the canonical orientation can be seen as the direction in which the surface bends the most

.

C. Feature Description

The feature descriptor summarizes the local neighbourhood around a keypoint. Therefore, it provides for each keypoint (with assigned scale and canonical orientation) a feature vector consisting of concatenated histograms. Each of these histograms is calculated over one of the nine small circular regions, defined with respect to the canonical orientation as shown in figure 1. The regions each have a geodesic radius of 3.75σ_s and their centres are located at a geodesic distance of 4.5σ_s (regions 2,4,6 and 8) or 4.5√2σ_s (regions 3,5,7 and 9) respectively, to the keypoint. In each region two histograms $\vec{p}_s$ and $\vec{p}_\theta$ with 8 bins each are computed. The first histogram contains the shape index, which is expressed for vertex i as

$$S_i = \frac{2}{\pi}\tan^{-1}\left(\frac{k_{i,1} + k_{i,2}}{k_{i,1} - k_{i,2}}\right) \quad (5)$$

with ki,1 the maximum and ki,2 the minimum curvature. The second contains the slant angles, which are defined as the angle between every projected normal and the canonical orientation. First, each entry (the shape index or slant angle of a vertex) for both histograms is Gaussian weighted with the geodesic distance to the key point (large circle in figure 2, σ = 4.5σ_s) and with the geodesic distance to the center of the region (small circles in figure1, σ =4.5σ_s). Moreover, the entries of the shape index histogram are weighted with the curvedness.

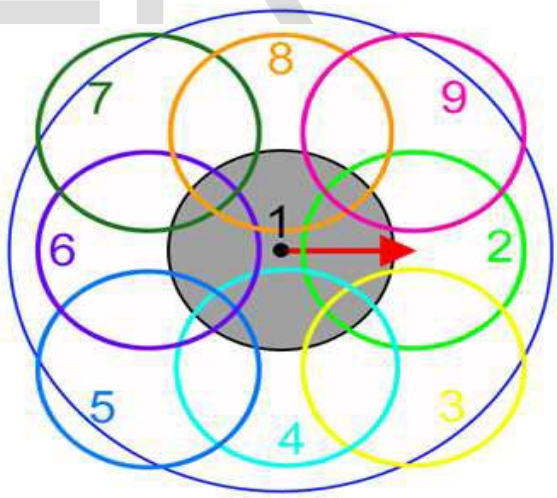

Fig:2: Location and order of the region w.r.t the canonical orientation.

used for the construction of the feature vector.($C = \sqrt{2H^2 - k}$) and the entries of the slant angle histogram are weighted with the tilted angle, i.e. the angle between the normal in the considered vertex and the normal in the keypoint. Next, every histogram is normalized and clipped to 1/√8 reducing the influence of large histogram values. Finally, the histograms are concatenated in a single feature vector $f_i = \left[\vec{p}S,1, \vec{p}\theta,1 \ldots\ldots\ldots \vec{p}S,9, \vec{p}\theta,9\right]^T$. A feature descriptor is

computed for each keypoint, resulting in a set of feature vectors per (face) surface F = {f1, f2, . . . fn}.

VI. CREATING GALLERY

To create gallery or gallery dictionary, for each sample scan in the gallery, first its local descriptors are computed by meshSIFT. Secondly these computed local descriptors for each scan are concatenated each other, this forms the gallery dictionary.

Given a probe 3D face scan, first the n number of keypoints are detected and for each keypoint si its local descriptor is computed. To compute features for single scan all the local descriptor for all keypoints of that scan are concatenated first as follows.

$$S = [s_1, s_2 \ldots\ldots\ldots\ldots s_n]$$

Consider there are N subjects in gallery and for each subject i there are totally ni derived descriptors. Usually, these ni descriptors are obtained from multiple samples of the subject i For the ith subject, let

$$\mathbf{G}i = [\boldsymbol{S}_{i,1}, \boldsymbol{S}_{i,2}, \ldots, \boldsymbol{S}_{i,}n_i] \in \mathbb{R}^{m\times n}i \quad (6)$$

where m here stands for the descriptor dimension. The gallery dictionary G can be simply constructed by concatenating these G is as:

$$\mathbf{G} = [\mathbf{G}1, \mathbf{G}2, \ldots, \mathbf{G}_N] \in \mathbb{R}^{m\times K} \quad (7)$$

where K here represents the total number of descriptors in the gallery set. G is the complete gallery set. Typically, K is very large, making G an over complete description space of the N classes.

VII.CLASSIFICATION USING SPARSE REPRESENTATION CLASSIFIER

Given a probe 3D face scan, we at first compute from it a set of local descriptors using (6).

We consider the problem of automatically recognizing human faces from 3D scan with varying expression and poses, as well as occlusion. We cast the recognition problem as one of classifying among multiple linear regression models and use sparse representation classifier that offers the key to addressing this problem.

With n the number of keypoints detected from this scan. Then, the sparse representation problem is formulated as:

$$\hat{X} = \arg\min_{x} \sum_{i=1}^{n} \| x_i \|_0 \; s.tS = GX \quad (9)$$

$\mathbf{X} = (\boldsymbol{x}1, \boldsymbol{x}2 \ldots\ldots\ldots\ldots \boldsymbol{x}n) \in \mathbb{R}^{K\times n}$ is the sparse coefficient matrix, and $||.||0$ denotes the l0-norm of a vector. However, the solution to this problem is NP-hard.

As suggested by the research results of compressed sensing [23], sparse signals can be well recovered with a high probability via the l1- minimization. Based on a sparse representation computed by 'l1-minimization, we propose a general classification algorithm. Therefore, Eq.(.9) can be approximated by:

$$\hat{X} = \arg\min_{x} \sum_{i=1}^{n} \| x_i \|_1 \; s.tS = GX \quad (10)$$

Where $||.||_1$ represents the l1-norm of the vector. This is a multitask problem as both X and S have multiple columns. Equivalently, we can solve the following set of n l1-minimization problems, one for each probe descriptor yi:

$$\hat{X}_i = \arg\min_{x_i} \| x_i \|_1, s.ts_i = Gx_i, i = 1, 2 \ldots n \quad (11)$$

To solve Eq.(3.11), we use the Homotopy algorithm proposed in [24]. Usually, if the identity of the probe face scan is covered by the gallery set, the coefficient vectors of its local descriptors would be very sparse.

Inspired by [24, 25], we adopt the following multitask SRC to calculate of the n descriptors with respect to each class to determine the identity of the input face scan.

$$r_i(S) = \sum_{i=1}^{n} \| s_i - G\partial_n(\hat{x}_i) \|_2 \quad (12)$$

where $\partial_n(\hat{x}_i)$ is a function which selects only the coefficients corresponding to class n.

After computing residual, the minimum value of residual is selected as the identity of probe scan S.

$$\text{Identity}(S) = \arg\min r_i(S) \quad (13)$$

VIII. EXPERIMENTAL RESULTS

A. Experiments on Bosphorus

The Bosphorus database [26] consists of 4666 facial range scans from 105 different subjects. In Bosphorus, facial expression variations, pose variations, and occlusions are present. The majority of the subjects are aged between 25 and 35. In our experiment, we chose 3 face scans with neutral expressions to form the gallery set, making the gallery set have 315 samples.

Herewe used 24 images from Gavab database as true negative samples. we have tested the results on Bosphorus database and achieved approximate 92.45% accuracy on same. In our experiment, we chose 3 face scans with neutral expressions to form the gallery set, making the gallery set have 315 samples. When forming the test set, 6 cases were considered. In the first case, the test set included all the samples containing expressions, in the second case the test set only occluded samples, third test set included all samples containing pose variations, forth test set contains all samples with various poses except 90 degree rotated samples, fifth test set contains all frontal samples in entire database containing that consist of all samples with expression, occlusion and samples with various poses, sixth test set contains all samples in entire database containing that consist of all samples with expression, occlusion and samples with various poses. The accuracy of proposed approach under all these test sets are listed in Table 1.

TABLE 1: RECOGNITION RATES OF PROPOSED APPROACH ON BOSPHORUS DATABASE UNDER DIFFERENT TEST CASES.

Sr. No	Approach(Test Set)	Gallery Size	Test Size	Recognition Rate
1	Expression(all)	315	2616	97.32%
2	Occlusion(all)	315	420	93.33%
3	Pose Variation(all)	315	1315	83.26%
4	PoseVariation(except 90 degree rotations)	315	1155	96.62%
5	Overall Database	315	4375	92.45%
6	Overall Database(except 90 degree Rotation)	315	4165	95.76%
7	Overall Database(Frontal)	315	3567	98.26%

We have also compared the results of proposed approaches with several other approaches. The identification results in terms of rank-1 recognition rate are summarized in Table 2.

TABLE 2: COMPARISON OF RECOGNITION RATES ON BOSPHORUS DATABASE.

Sr. No	Approach	Galley Size	Test Size	Recognition Rate
1	Proposed Approach(all)	315	4375	92.45%
2	Proposed Approach(frontal)	315	3567	98.26%
3	Smeets et al.[2](all)	315	4351	92.99%
4	Smeets et al.[2](frontal)	315	3543	96.56%
5	Alyuzet al. [27](frontal)	47	1508	95.3%
6	ICP [28](frontal)	47	1508	72.40%
7	Dibekliogluet al. [29] (frontal)	47	1508	89.2%
8	Hajatiet al. [30](all)	-	-	69.1%
9	HassenDriraet al.[31](all)	-	-	89.25%

IX.CONCLUSION

In this work, we have presented a framework for recognition of 3D faces under large facial expression, occlusions and pose variations. We have also presented literature survey and system development strategy for 3D face recognition designed to handle variations of facial expression, pose variations, and occlusions between gallery and probe scans. In proposed system given a probe face its features are extracted using meshSIFT algorithm as a multiple point descriptor and then these features are compared with gallery faces using sparse classifier. If the probe face belongs to gallery face its identity would be very sparse than other faces in the gallery. The proposed system is able to properly recognize the faces having large facial expression, occlusion and pose variations.

Using this approach we got 92.45% accuracy on all images Bosphorus database and 98.26% accuracy on frontal images of same database. Bosphorus is the most prominent database of 3D faces, consist of 3D images with large facial expression(consist of 6 basic expression such as smile, anger etc. and number facial action units), occlusion(such as hair, glasses, mouth etc) and pose variations(cross rotation, pitch rotation, yaw rotation with varying degree of rotation ranged from 10◦ to 90◦).

REFERENCES

[1] Hassen D, Boulbaba B, Member, IEEE, AnujSrivastava, Senior Member, I EEE, Mohamed Daoudi, Senior Member, IEEE, and Rim Slama,"3D face recognition under expression, occlusion and pose variation" *IEEE Transactions On Pattern Analysis And Machine Intelligence*, Vol. 35, No. 9, September 2013.

[2] A.M.A. Bronstein, M.M.M. Bronstein, and R. Kimmel, "Three-Dimensional Face Recognition," *Int'l J. Computer Vision*, vol. 64, no. 1, pp. 5-30, 2005.

[3] Samir C, Srivastava A, Daoudi M, Klassen E (2009) An intrinsic framework for analysis of facial surfaces. *International Journal of Computer Vision* 82: 80-95.

[4] Bronstein AM, Bronstein MM, Kimmel R (2007) Expression-invariant representations of faces. *IEEE Transactions on Image Processing* 16: 188-197.

[5] Y. Lee, H. Song, U. Yang, H. Shin, and K. Sohn, "Local Feature Based 3D Face Recognition," *Proc. Audio- and Video-Based Biometric Person Authentication*, pp. 909-918, 2005.

[6] S. Gupta, J.K. Aggarwal, M.K. Markey, and A.C. Bovik, "3D Face Recognition Founded on the Structural Diversity of Human Faces," *Proc. IEEE Conf. Computer Vision and Pattern Recognition*, 2007. pp. 1008-1116.

[7] T.C.T. Faltemier, K.W.K. Bowyer, and P.J.P. Flynn, "A Region Ensemble for 3D Face Recognition," *IEEE Trans. Information Forensics and Security*, vol. 3, no. 1, pp. 62-73, Mar. 2008.

[8] G. Gordan, "Face Recognition Based on Depth and Curvature Features," Proc. *IEEE Conf. Computer Vision and Pattern Recognition*, pp. 108-110,1992.

[9] R. McKeon and T. Russ, "Employing Region Ensembles in a Statistical Learning Framework for Robust 3D Facial Recognition," *Proc. Fourth IEEE Int'l Conf. Biometrics: Theory Applications and Systems*, pp. 1-7, 2010.

[10] Kakadiaris I, Passalis G, Toderici G, Murtuza M, Lu Y, et al. (2007) Three-dimensional face recognition in the presence of facial expressions: An annotated deformable model approach. *IEEE Transactions on Pattern Analysis and Machine Intelligence* 29: 640-649.

[11] C.C.C. Queirolo, L. Silva, O.R.O. Bellon, and M.P.M. Segundo, "3D Face Recognition Using Simulated Annealing and the Surface Interpenetration Measure," *IEEE Trans. Pattern Analysis and Machine Intelligence*, vol. 32, no. 2, pp. 206-219, Feb. 2010.

[12] N. Alyuz, B. Gokberk, and L. Akarun, "A 3D Face Recognition System for Expression and Occlusion Invariance," *Proc. Second IEEE Int'l Conf. Biometrics: Theory, Applications and Systems*, 2008.

[13] Berretti S, Bimbo AD, Pala P (2010) 3D face recognition using isogeodesic stripes. *IEEE Transactions on Pattern Analysis and Machine Intelligence* 32: 2162-2177.

[14] Mahoor MH, Abdel-Mottaleb M (2009) Face recognition based on 3D ridge images obtained from range data. *IEEE Transactions on Pattern Recognition* 42: 445-451.

[15] Drira H, Amor BB, Srivastava A, Daoudi M, Slama R (2013) 3D face recognition under expressions, occlusions, and pose variations. *IEEE Transactions on Pattern Analysis and Machine Intelligence* 35: 2270-2283.

[16] A. Jain, X. Lu, and D. Colbry, "Three-dimensional model based face recognition," Proc. *17th International Conference on Pattern Recognition*, vol. I, pp. 362–366, 2004.

[17] K.Chang, K. W. Bowyer, and P. Flynn, "Multiple nose region matching for 3D face recognition under varying facial expression," *IEEE Transactions on Pattern Analysis and Machine Intelligence*, pp. 1–6, 2006.

[18] G. Passalis, P. Perakis, T. Theoharis, and I.A.I. Kakadiaris, "Using Facial Symmetry to Handle Pose Variations in Real-World 3D Face Recognition," *IEEE Trans. Pattern Analysis and Machine Intelligence*, vol. 33, no. 10, pp. 1938-1951, Oct. 2011.

[19] X. Lu and A. Jain, "Deformation Modeling for Robust 3D Face Matching," IEEE *Trans. Pattern Analysis and Machine Intelligence*, vol. 30, no. 8, pp. 1346 -1357, Aug. 2008.

[20] Lowe DG (2004) Distinctive image feature from scale-invariant keypoints. *International Journal of Computer Vision* 60: 91-110.

[21] Smeets D, Keustermans J, Vandermeulen D, Suetens P (2013) MeshSIFT: Local surface features for 3D face recognition. *Computer Vision and Image Understanding* 117: 158-169.

[22]. Geng C., Jiang X.: SIFT features for Face Recognition, *IEEE Conference CSIT*, pp. 598–602, 2009.

[23] S. Chen, D. Donoho, and M. Saunders, "Atomic Decomposition by Basis Pursuit," *SIAM Rev.*, vol. 43, no. 1, pp. 129-159, 2001.

[24] D. Donoho and Y. Tsaig, "Fast Solution of '1-Norm Minimization Problems when the Solution May Be Sparse," *preprint,http://www.stanford.edu/~tsaig/research.html, 2006.*

[25] D. Donoho, "Neighborly Polytopes and Sparse Solution of Underdetermined Linear Equations," *Technical Report 2005-4, Dept. of Statistics*, Stanford Univ., 2005.

[26] Bosphorus: *Bosphorus.ee.boun.edu.tr/*

[27] Alyuz N, Gokberk B, Dibekliglu H, Savran A, Salah AA, et al. (2008) 3D face recognition benchmarks on the Bosphorus database with focus on facial expressions. *Proceedings of the BIOID*, pp. 1-7.

[28] Alyuz N, Gokberk B, Akarun L (2008) A 3D face recognition system for expression and occlusion invariance. *Proceedings of the BTAS*, pp. 1-7

[29] Dibekliglu H, Gokberk B, Akarun L (2009) Nasal region based 3D face recognition under pose and expression variations. *Proceedings of the ICB*, pp. 309-318.

[30] Hajati F, Raie AA, Gao Y (2012) 2.5D face recognition using patch geodesic moments. *Pattern Recognition* 45: 969-982.

[31] Hassen D, Boulbaba B, Member, IEEE, AnujSrivastava, Senior Member, IEEE, Mohamed Daoudi, Senior Member, IEEE, and Rim Slama,"3D face recognition under expression, occlusion and pose variation" *IEEE transactions on pattern analysis and machine intelligence*, VOL. 35, NO. 9, SEPTEMBER 2013.

[32] C. Maes, T. Fabry, J. Keustermans, D. Smeets, P. Suetens, and D. Vandermeulen, "Feature detection on 3D face surfaces for pose normalisation and recogntiion," in BTAS '10, *IEEE Int. Conf. on Biometrics: Theory, Applications and Systems*, pp. 1-6, September 2010, Washington D.C., USA.

[33] D. Smeets, J. Keustermans, J. Hermans, P. Claes, D. Vandermeulen, P. Suetens, "Symmetric surface-feature based 3D face recognition for partial data," in IJCB '11: *The International Joint Conference on Biometrics*, pp. 1-5, October 11-13, 2011, Washington D.C., USA.